Supplementary Information for:

The C-terminal activating domain promotes Panx1 channel opening

Erik Henze[1†], Jacqueline J. Ehrlich[1†], Janice L. Robertson[2†], and Toshimitsu Kawate[1*]

[1]Department of Molecular Medicine, Cornell University, Ithaca, NY 14853, USA
[2]Department of Biochemistry and Molecular Biophysics, Washington University School of Medicine, St. Louis, MO 63110, USA

[†]These authors contributed equally to this work.

*Corresponding author:

Toshimitsu Kawate
Department of Molecular Medicine
Cornell University
C4-151 VMC, 930 Campus Rd, Ithaca, NY 14853
Email: toshi.kawate@cornell.edu
Phone: 607-253-3783

The supplementary information includes: Figures S1 to S7, Table S1-2

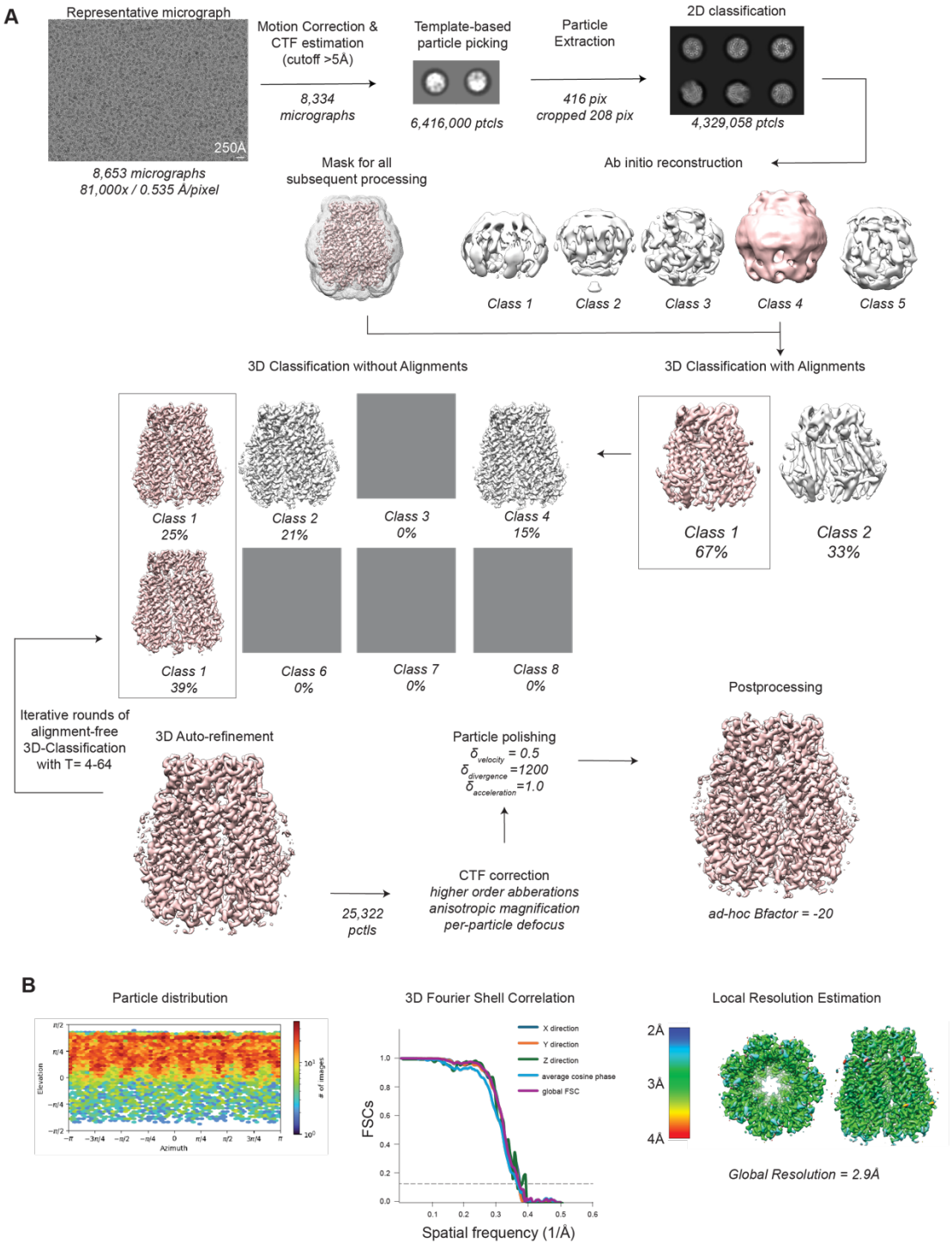

Fig. S1 (A) Cryo-EM data processing workflow for frPanx1-ΔC. Initial micrograph processing was carried out in Relion 4.0 (52), then moved to cryoSPARC 4.0 (45) for 2D classification. Particles were moved back to Relion for 3D classification and final map refinement. Model fitting was performed with Coot (46) and model refinement was done with Phenix. Tau-fudge parameters executed in sequence to isolate highest resolution particles are T=4, T=8, T=16, T=32, and T=64 with a 3D-autorefinement job in between each. (B) Refinement statistics for frPanx1-ΔC maps. Particle distribution and local resolution (cutoff 0.143) maps from cryoSPARC. 3DFSC charts were generated via the remote 3DFSC processing server hosted at the New York Structural Biology Center (53).

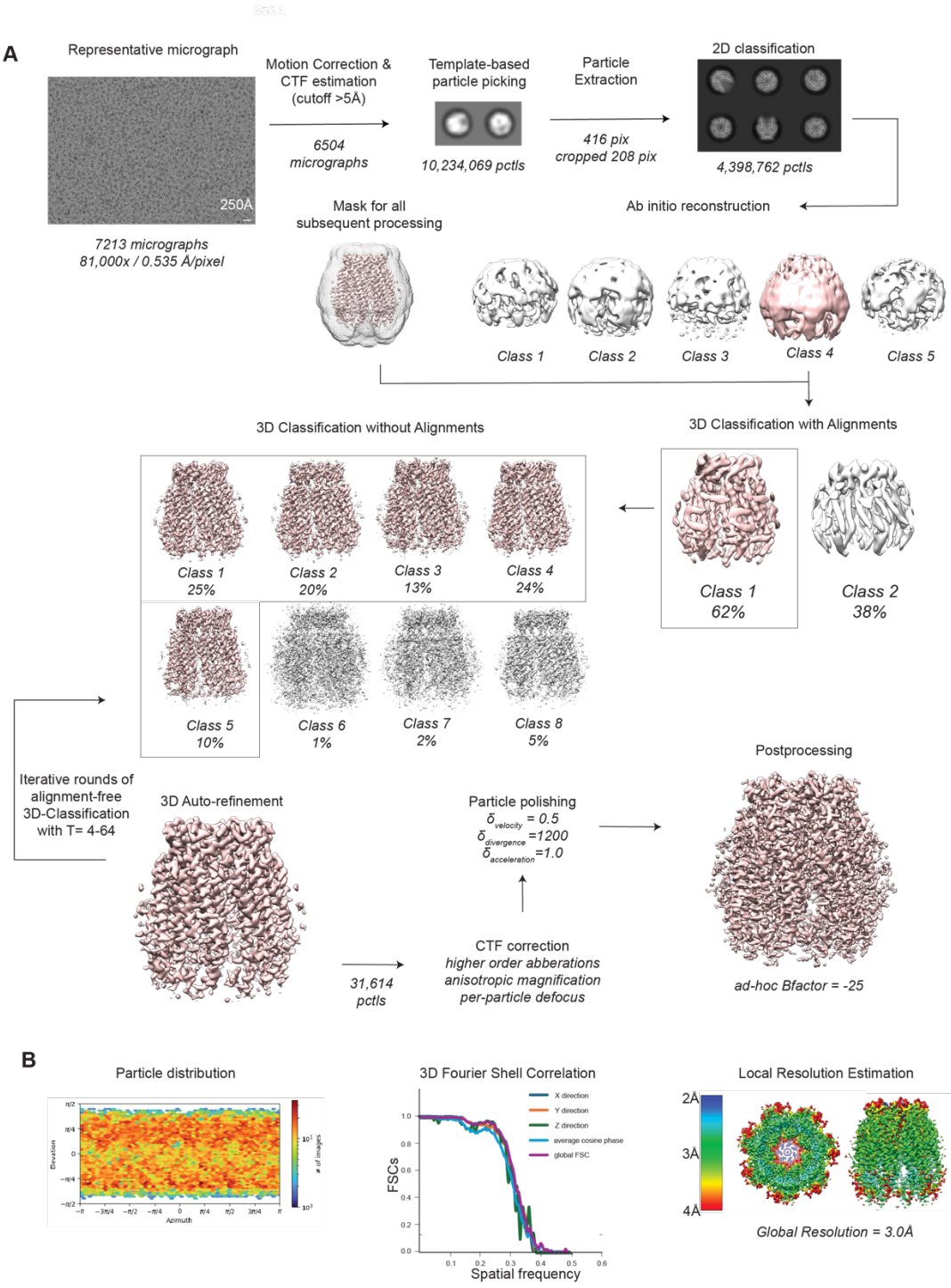

Fig. S2 (A) Cryo-EM data processing workflow for frPanx1-ΔC+CAD. Initial micrograph processing was carried out in Relion 4.0 (52), then moved to cryoSPARC 4.0 (45) for 2D classification. Particles were moved back to Relion for 3D classification and final map refinement. Model fitting was performed with Coot (46) and model refinement was done with Phenix. Tau-fudge parameters executed in sequence to isolate highest resolution particles are T=4, T=8, T=16, T=32, and T=64 with a 3D-autorefinement job in between each. (B) Refinement statistics for frPanx1-ΔC+CAD maps. Particle distribution and local resolution (cutoff 0.143) maps from cryoSPARC. 3DFSC charts were generated via the remote 3DFSC processing server hosted at the New York Structural Biology Center (53).

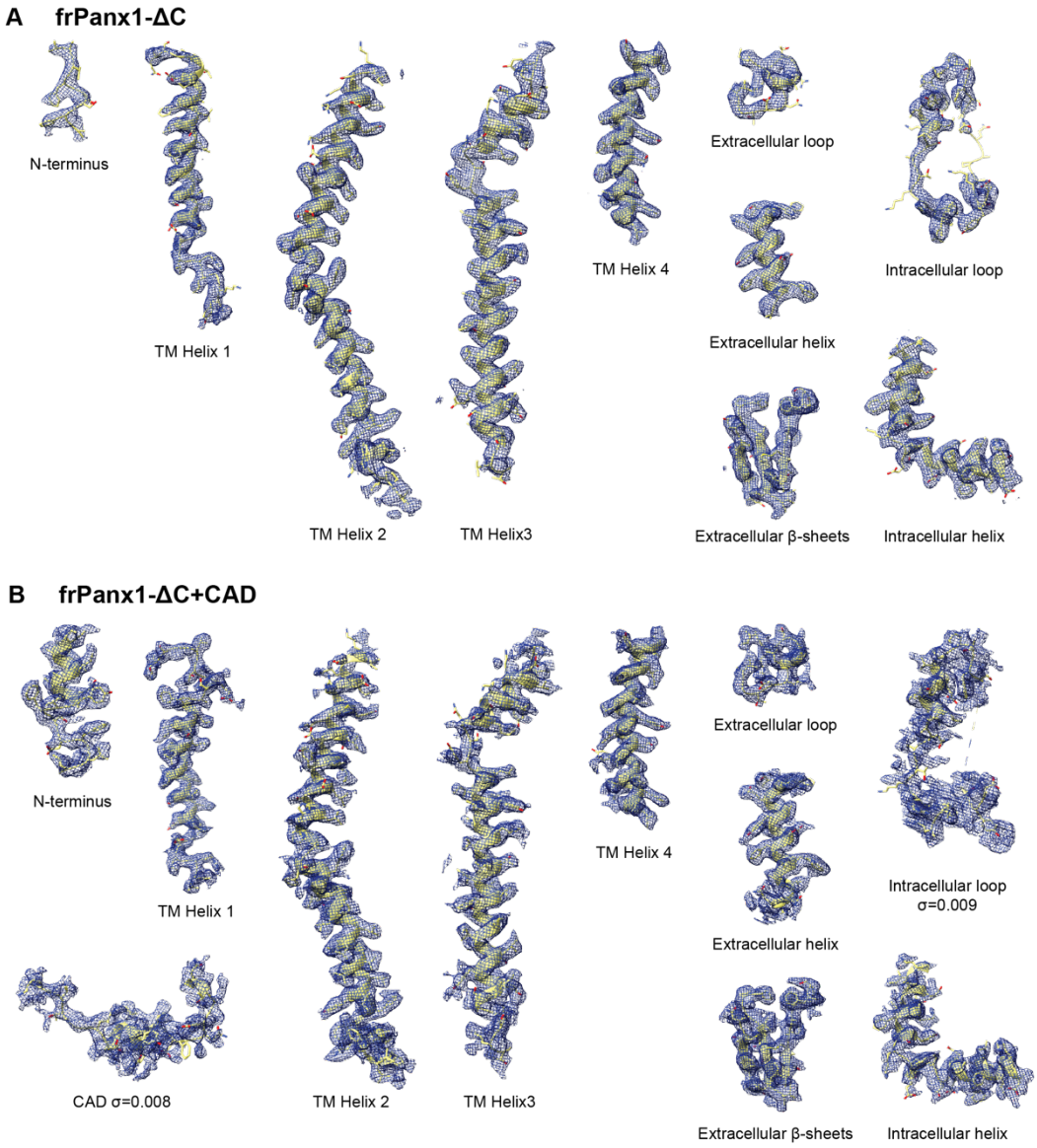

Fig. S3: Cryo-EM density at different parts of frPanx1. The models are fit into the cryo-EM maps of frPanx1-ΔC (A) and frPanx1-ΔC+CAD (B). Thresholds for maps are 0.01 and 0.013, respectively, unless otherwise noted.

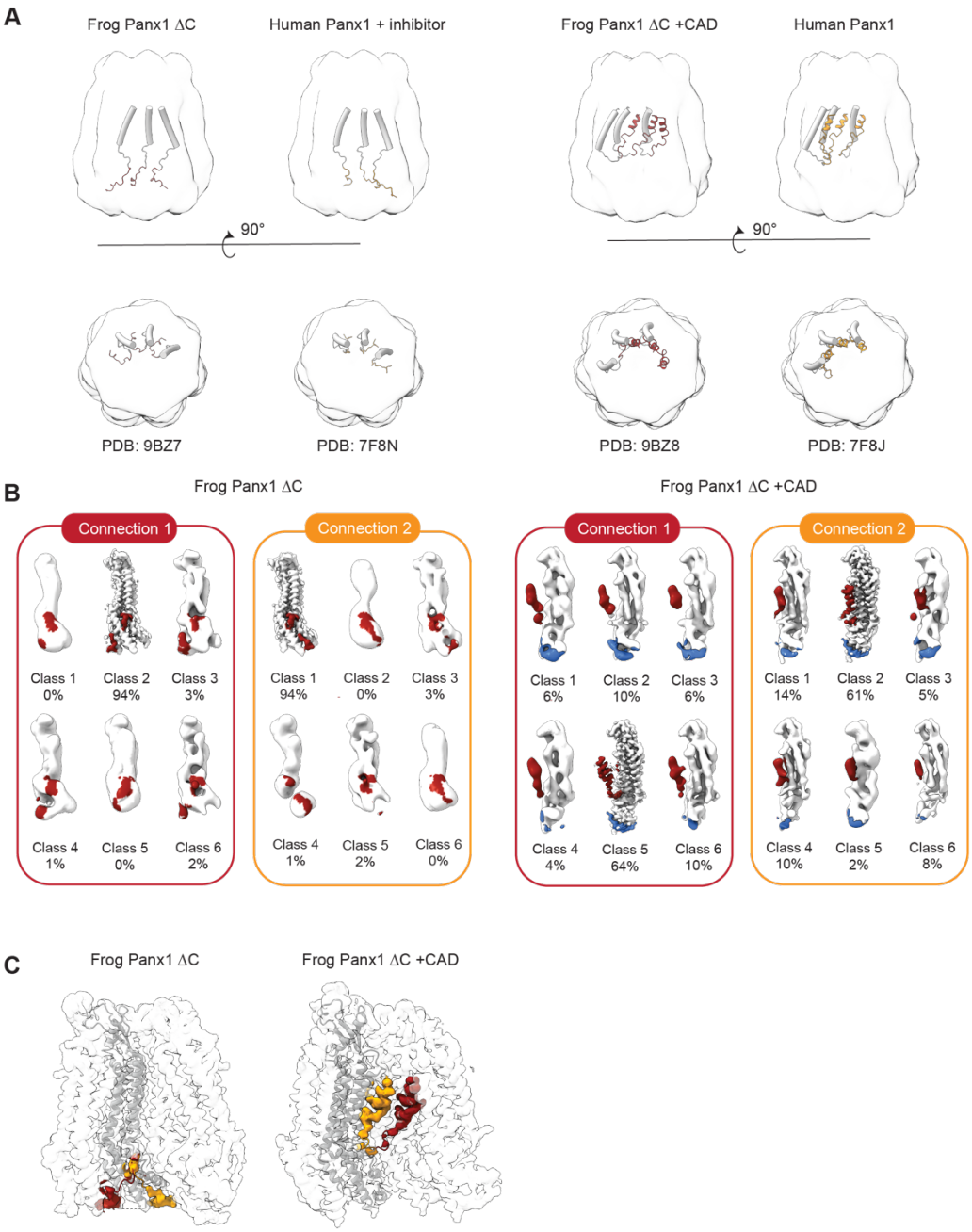

Fig. S4: Structural comparison of the Panx1 structures. (A) Structures of human and frog Panx1 orthologs have consistent architecture in closed and open or primed conformations with a heptameric assembly and the narrowest constriction located at W74. Structures obtained from this study are shown in red and previously reported structures from Kuzuya et al (30) are shown in blue. Top view is from the extracellular side perpendicular to the plasma membrane and side views are taken parallel to the membrane. (B) Cryo-EM data processing results of single protomers from 3D classification. Maps were generated for each N-terminal connection and the same batch of particles were subject to particle subtraction and 3D classification to better visualize the density connecting the N-terminus to the first TM helix. (C) Comparison of the possible N-terminal positions in both constructs. Density highlighted in red was used for modeling the structures from this paper, and densities highlighted in orange is the reported connection by Kuzuya et al.

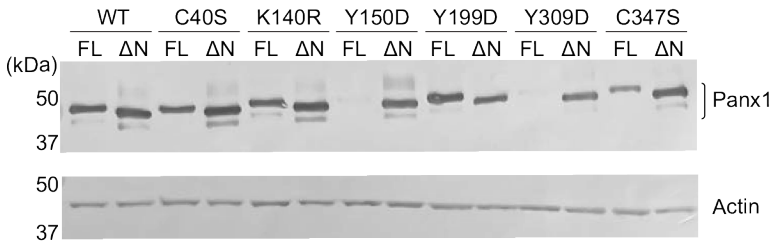

Fig. S5: Surface expression levels of PTM mutants. Surface-biotinylated Panx1 PTM mutants were pulled down and detected by western blot using anti FLAG antibody. Anti-actin antibody was used to control the loading amount. The target proteins were detected by colorimetric method using alkaline phosphatase substrates.

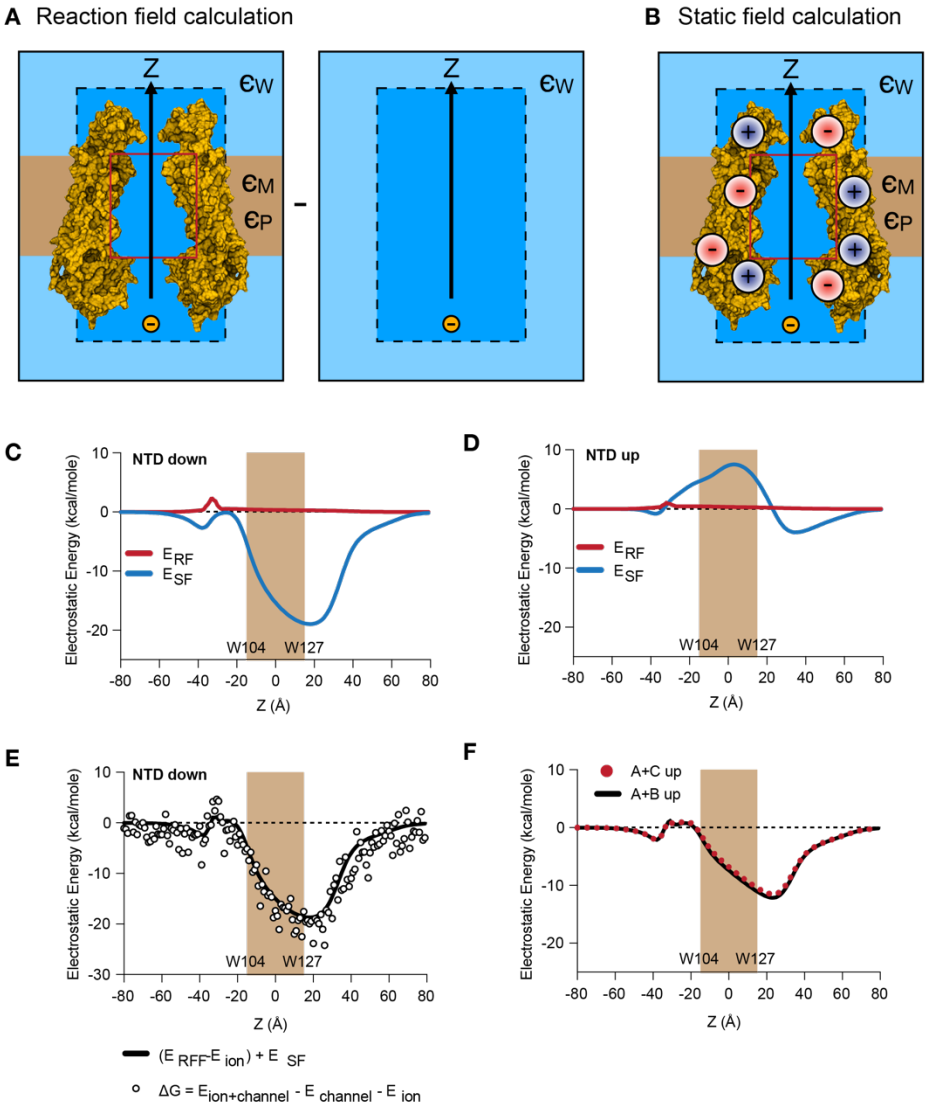

Fig. S6: Continuum electrostatics calculations. (A) In a continuum Poisson-Boltzmann calculation, the water/protein/membrane system is defined along a 3D grid and solved using the PBEQ module in CHARMM. The water, protein and membrane dielectrics are represented as ϵ_W, ϵ_P, and ϵ_M respectively. In addition, there is a cylinder representation (red box) that allows for the dielectric environment inside the pore to be set to ϵ_W. The dashed line defines an additional box, so that ionic screening is considered only outside of the pore. The solid arrow indicates the axis of ion permeation, defined along Z. The reaction field contribution to the electrostatic interaction free energy is calculated by solving for the ion in the field of the protein/membrane dielectric environment with all charges turned off (E_{RFF}) and subtracting the ion alone in the box (E_{ion}), where $A = E_{RFF}-E_{ion}$. (B) The protein static field contribution is calculated by solving the field in 3D space due to the protein charges in the dielectric environment. (C) The energy due to the reaction field is calculated *as* $E_{RF} = ½ AQ^2$ and static field $E_{SF} = BQ^2$. E_{RF} and E_{SF} for the NTD down structure of frPanx1 and (D) NTD up structure that includes the CAD. (E) A comparison of the two approaches to calculating the interaction energy of the ion inside of the pore, $E_{RF}+E_{SF}$ (line) and $\Delta G_{int.} = E_{ion+channel} – E_{channel} - E_{ion}$ (points), showing overlap. The noise in the latter calculation arises from variability in the solution when moving the ion along Z in the $E_{ion+channel}$ calculation. (F) Comparison of $E_{RF}+E_{SF}$ in the hybrid models where A+B vs. A+C subunits were made with the NTD in the up position, showing similar electrostatic profiles.

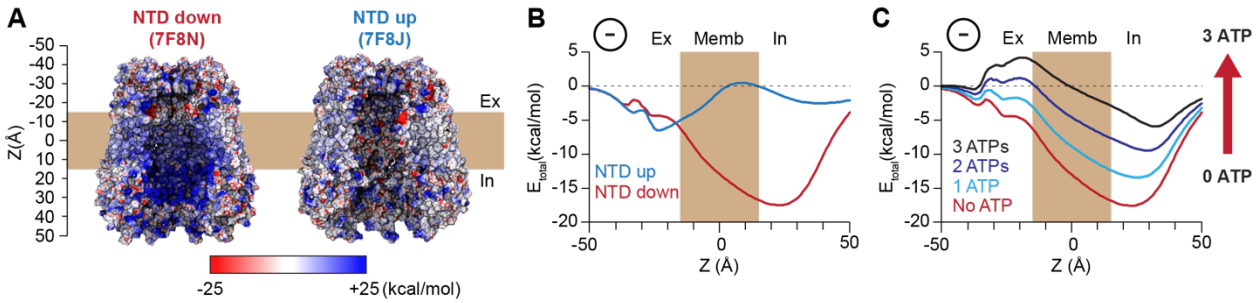

Fig. S7: Electrostatic energy landscape of the human Panx1 channel. (A) Electrostatic surface potential of a coronal section of the frPanx1-ΔC (left) and frPanx1-ΔC+CAD (right) ion permeation pathway. Electrostatic surface potential was calculated using CHARMm-PBEQ (1) and presented in the range between -25 kcal/mol (red: acidic) and +25 kcal/mol (blue: basic). (B) Electrostatic contribution for an anion binding free energy (E_{total}) along the permeation pathway (z=0 in the middle of predicted transmembrane) for the 7F8N (red) and 7F8J (blue), and hybrid models harboring 0-7 NTDs (C) Electrostatic free energy calculation of 7F8N (red) in the presence of 0-3 ATP molecules in the deep energy well. Calculations are carried out using CHARMM-PBEQ module to solve the Poisson-Boltzmann solution of the system.

Table S1. Statistics for reconstructions and model building

Codes	frPanx1-ΔC PDB: EMDB:	frPanx1-ΔC+ CAD PDB: EMDB:
Data collection and processing		
Microscope	Titan Krios	Titan Krios
Camera	K3 BioQuantum	K3 BioQuantum
Magnification	81,000x	81,000x
Voltage (kV)	300	300
Defocus Range	-1.0 to -2.0	-1.0 to -2.0
Exposure time	3.81	3.83
Total dose	50	50
Number of frames	50	50
Pixel size	1.07 (0.535 in super-resolution)	1.07 (0.535 in super-resolution)
Micrographs (no.)	8334	6504
Symmetry imposed	C7	C7
Initial particles (no.)	6,416,000	10,234,069
Final particles (no.)	25,322	31,614
Map resolution (Å)	2.9	3.0
FSC threshold	0.143	0.143
Refinement		
Initial model (PDB code)	6VD7	6VD7
Model resolution (Å)	3.1	3.0
FSC threshold	0.5	0.5
Model composition		
Non-hydrogen atoms	16,961	18,277
Protein residues	2,086	2,254
Ligands	0	0
B factors (Å^2)	-20	-25
R.m.s deviation		
Bond length (Å)	0.002	0.002
Bond angle (°)	0.544	0.511
Validation		
Favored (%)	95.89	97.77
Allowed (%)	4.11	2.23
Disallowed (%)	0	0
Rotamer outliers (%)	1.84	2.73
MolProbity score	1.95	1.79
Clash score	8.74	7.34

Table S2 Parameters for PBEQ calculations. All other parameters are set to default values.

Variable	**Value**	**Physical meaning**
(NCELX,NCELY,NCELZ)	frPanx1-ΔC: (289, 287, 397)	Number of grid points
DCEL1	1.0 Å	Coarse grid dimension
DCEL2	0.5 Å	Focusing grid dimension
(XBCEN,YBCEN,ZBCEN)	(0 Å, 0 Å, 0 Å)	Center of box
EPSP	2	Protein dielectric constant
EPSW	80	Water dielectric constant
CONC	0.15 M	Ionic concentration where allowed
WATR	1.4 Å	Solvent probe radius
IONR	0.0 Å	Ion exclusion radius
TEMP	300 K	Temperature
ZMEMB	0 Å	Center of membrane
TMEMB	30 Å	Membrane thickness
EPSM	2	Membrane dielectric constant
RCYLN	15 Å	Radius of cylinder to form aqueous pore across membrane
HCYLN	30 Å	Height of cylinder across membrane
EPSC	80	Cylinder dielectric
(XCYLN,YCYLN,ZCYLN)	(0 Å, 0 Å, 0 Å)	Center of cylinder
(LXMIN,LYMIN,LZMIN)	(-25 Å, -25 Å. -55 Å)	Minimum box dimensions
(LXMAX, LYMAX,LZMAX)	(25 Å, 25 Å, 65 Å)	Maximum box dimensions
EPSB	80	Box dielectric (except protein)